Program Digest, 2019 IEEE International Ultrasonics Symposium (IUS)
Glasgow, Scotland, October 6-9, 2019

Optimal Blind-Source-Separation Filtering for Ultrasound Clutter Suppression: Application to Ultrasound Localization Microscopy and Speckle Tracking

R.R. Wildeboer[1], F. Sammali[1], R.J.G. van Sloun[1], H. Wijkstra[1,2], and M. Mischi[1]

[1]Dept. of Electrical Engineering, Eindhoven University of Technology, The Netherlands
[2]Dept. of Urology, Amsterdam University Medical Centers, University of Amsterdam, Amsterdam, The Netherlands

***Abstract*—Ultrasound localization microscopy (ULM) exploits microbubbles to generate super-resolution images beyond the diffraction limit, and ultrasound speckle tracking (UST) allows for the estimation of tissue motion and strain. For both applications, suppression of noise and clutter is essential. This is effectively achieved using blind source separation techniques such as singular value decomposition, but given the limitations of heuristic subspace selection, useful criteria that enable automatic and adaptive selection of the desired signal components should be established. In this work, synthetic ultrasound data was used to test a comprehensive range of (proposed and novel) effective criteria based on domain knowledge for adaptive signal subspace selection for ULM and UST. For ULM, tissue clutter is most effectively suppressed by removing singular components with a mean spectral density above a frequency threshold. Also for UST, identification of signal singular components by spectral thresholding proved to be the most effective. Even though its performance for *in-vivo* acquisitions remains to be investigated, the proposed method shows promise for adaptive clutter suppression.**

***Index Terms*—Blind Source Separation, Singular Value Decomposition, Ultrasound Localization Microscopy, Ultrasound Speckle Tracking**

I. Introduction

Ultrasound localization microscopy (ULM) and ultrasound speckle tracking (UST) are examples of advanced ultrasound (US) imaging applications. More specifically, ULM is used to generate super-resolution images, that is, images in which microbubbles (i.e., US contrast agents) are localized with a precision beyond the diffraction limit [1], [2]. This technique, inspired by optical super-localization techniques [3], is especially useful to map vascular architectures. UST, on the other hand, makes use of the inherent speckle patterns found in US imaging to track global and local tissue motion. UST has a well-established echocardiographic application [4], [5], but can also be applied for vector flow imaging [6] or quantitative assessment of uterine motion outside pregnancy [7].

Data preprocessing is essential to the application this type of algorithms, since their outcomes for a great part rely on the quality of the input US data. The suppression of clutter and noise is a significant part of this pipeline. The removal of these undesired signals is traditionally carried out using temporal and spatial filtering [8], [9], mostly through (in)finite response filters. However, these can only be effectively applied when clutter and noise are found in different spectral bands than the desired signal [10]–[12]. When this criterion is not met, the filtering technique might remove useful information or fail to suppress artefacts in the signal, and consequently hamper robust and effective the application of the aforementioned US techniques.

Recently, blind source separation (BSS) filtering has been introduced to ultrasound imaging [10]–[12], such as singular value decomposition (SVD) and independent component analysis. The advantage of BSS techniques is that they allow adaptive decomposition of the ultrasound signal into components with specific spatiotemporal behaviour rather than into specific (spatial) frequency bands. Even clutter and noise that spectrally overlap the desired signal can therefore be removed from the imaging. Central to BSS filtering is the identification of components that contain clutter or noise, or alternatively, that contain the desired signal. Although heuristic or empirical thresholds on the number of components to be included have been widely used [13]–[17], there is a demand for an adaptive, generalizable method for the identification of the desired signal components [10], [17], [18].

Adaptive BSS filtering for Doppler imaging of blood flow has extensively been studied [10], [12], [17], [18]; however, for ULM and UST the methods are still scarce. In this work, we evaluate a series of subspace selection methods for their effectiveness for ULM and UST, respectively. More specifically, we studied SVD filtering on a contrast-enhanced US cine-loop and an echocardiographic US video that were generated *in silico* and subsequently contaminated with known clutter and noise artefacts, so that a reliable ground truth was available.

II. Materials and Methods

A. Singular value decomposition filtering

SVD is a BSS technique that infers the decomposition from the signal itself by maximizing autocovariance [19]. Mathematically, SVD of a data matrix $\mathbf{X}$, in which all spatial locations are located along the rows and the temporal dimension is represented as columns, can be described as [20]

$$\mathbf{X} = \mathbf{U}\mathbf{\Sigma}\mathbf{V}^T, \tag{1}$$

where $\mathbf{U}$ and $\mathbf{V}$ represent the spatial and temporal singular vectors, respectively, and $\mathbf{\Sigma}$ contains the singular values along its diagonal. Through multiplication of the k^{th} column of $\mathbf{U}$ with the k^{th} singular value and the k^{th} row of $\mathbf{V}$, individual singular components can be constructed. A filtered image is eventually created by taking the sum of all desired singular components.

In this work, we test a comprehensive range of (proposed and novel) effective criteria based on domain knowledge for adaptive signal subspace selection. More specifically, the strategies to identify the components that contain the desired signal are based on information theory, noise modelling, sparsity, or spectral and spatial characteristics. Noise modelling and information theoretic criteria are mostly universal, based on e.g. the minimum description length [21] or Marčenko-Pastur modelling of noisy singular values [22].

For ULM specifically, we assume that tissue movement is slower and much more spatially coherent than blood motion [10], [18], [23]. We use domain knowledge to establish thresholds for the required spatial or temporal characteristics, i.e., a mean power spectral density of >10 Hz and spatial spectral density of >3.3 mm^{-1}. In addition, we select components based on their sparsity (as quantified through the normalized kurtosis as defined in [24]) or identify the signal regime by locating two "turning points" in the singular domain separating it from clutter and noise [18].

On the other hand, the UST movie is filtered such that the deterministic speckles patterns originating from anatomical structures are left unaltered while reducing the noise and clutter. For this, we define that the majority of the power spectral density should be between 0.5 and 1.5 Hz and the mean spatial spectral density above 0.1 mm^{-1}. Moreover, we also select components that exhibit strong periodicity (as quantified by the height of a non-zero-lag peak in the normalized autocorrelation trace).

B. Ultrasound localization microscopy

The simulated contrast-enhanced US video was generated by simulating the propagation of 26 microbubbles along a vascular network. Their backscattering coefficients were randomly generated and their speed was ~2 mm/s, typical for the blood velocity in a 5$^{\text{th}}$ generation microvascular vessel [25]. The clutter signal of tissue was constructed by randomly locating 500 scatters in the imaging domain that moved together at a speed of 0.2 mm/s, imaged in the same fashion as the

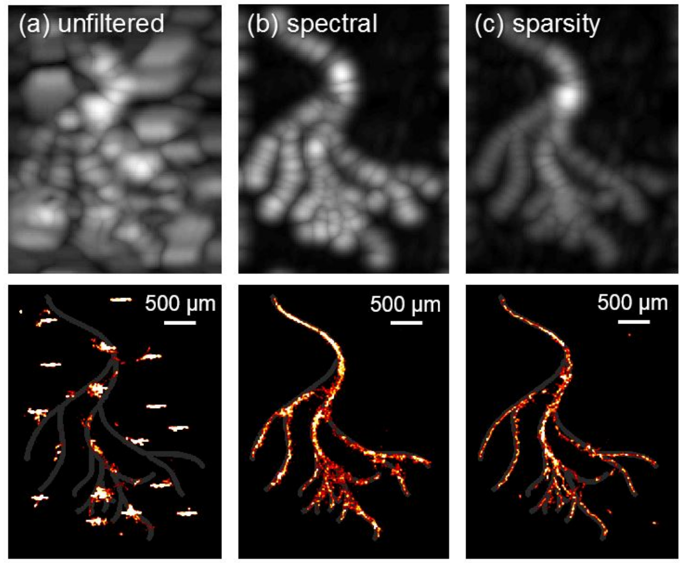

Fig. 1: Maximum-intensity projection and the corresponding super-resolved image of the (a) unfiltered data, (b) filtered data through spectral subspace selection, and (c) filtered data through component selection using a sparsity threshold.

microbubbles. Imaging was subsequently modelled by a scatter point-spread function of ~0.15 mm, modulated at 7-MHz. Finally, the simulation was generated with a frame rate of 400 Hz.

To evaluate the effectiveness of the proposed filtering, we implemented a standard ULM approach based on the localization of Gaussian point-spread function centroids [2]. As the performance is related to the ability to minimize the number of localizations outside the actual vasculature as well as the number of pixels inside the vessel that were not localized, we introduce the F_1-score as measure of filtering performance. This score is defined as

$$F_1 = \frac{2\text{TL}}{2\text{TL} + 2\text{FL} + \text{ML}}, \tag{2}$$

where TL, FL, and ML depict the number of true, false, and missed localizations.

C. Ultrasound speckle tracking

The *in-silico* construction of a synthetic phased-array echocardiographic video was based on a 3D finite-element model of a heart that was built to simulate the mechanical behaviour of the human heart during a cardiac cycle [26]. Exploiting the nodes in the finite-element model as US scatterers, a 2D four-chamber-view US recording was formed by a series of 161 diverging scan lines with an interline distance of 0.6°. Each line was generated by summing all scatterer contributions approximated by a four-cycle 2.5-MHz-modulated Fraunhofer-distributed pressure field. Clutter sources and Gaussian-distributed white noise were introduced in the RF date before demodulating the scan lines that made up the eventual 54-Hz 3-cycle heart video.

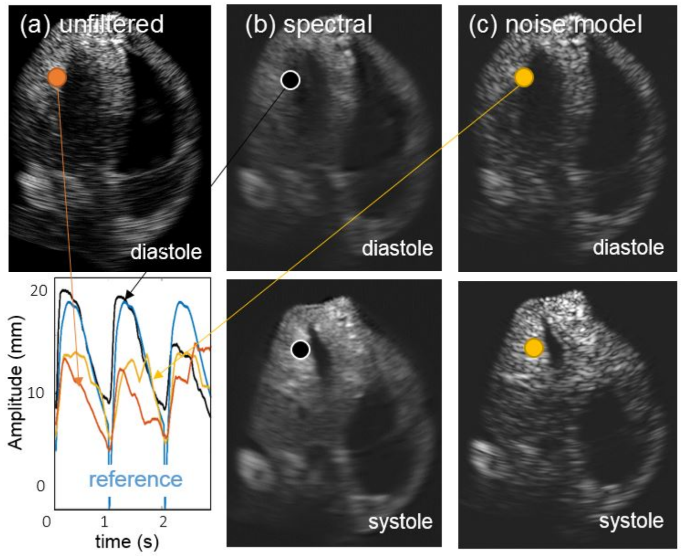

Fig. 2: Diastolic and systolic frame in the (a) unfiltered data, (b) filtered data through spectral subspace selection, and (c) filtered data through component selection based on noise modelling.

A pyramidal Lucas-Kanade optical flow method [27] was used for the frame-to-frame tracking of a specific speckle that could be directly associated with a finite-element node in the original cardiac model. This way, the motion (i.e., Euclidean distance from the scatterer or speckle to the initial position) as assessed by tracking was compared to the actual motion of the scatterer. Out-of-plane movement that relates to rotation and motion of the heart in the chest cavity was thus taken into account.

III. Results

A. Ultrasound localization microscopy

For SVD filtering of contrast-enhanced US imaging, we found that ULM reached the highest performance by spectral, turning-point, and sparsity-based criteria, with F_1-scores of 0.76, 0.73 and 0.72, respectively. No filtering or simple spectral filtering (also >10 Hz) yielded F_1-scores of 0.19 and 0.50. In Figure 1, the filtered images and corresponding ULM images are depicted.

B. Ultrasound speckle tracking

SVD filtering for UST in echocardiography performed best using noise modelling (i.e., a cumulative singular value threshold of 90%) and a spectral threshold. For these two criteria, the highest correlation coefficient (Pearson $r = 0.71\pm0.07$) and the lowest mean squared error (0.00048 ± 0.00032 mm^2) were found with reference to the ground truth movement. UST based on unfiltered data reached a Pearson r and mean squared error of only 0.64 ± 0.06 and 0.13 ± 0.1 mm^2, respectively.

IV. Discussion and Conclusion

Although BSS allows for adaptive filtering, subspace selection is still mostly carried out heuristically or empirically in US imaging. In this work, we have compared different strategies to identify those singular components containing signal and those containing noise or clutter. As signal quality may differ substantially between acquisitions [10], [18], a well-tailored adaptive subspace selection strategy would make BSS filtering more robust. We found that assessment of the spectral content of each component is in general the best way to select the appropriate signal components for both ULM and UST.

It must be emphasized that there is an intrinsic difference between spectral SVD filtering and standard temporal (in)finite response filters, since SVD is able to separate signal and noise information with a similar frequency content exploiting the statistical independence or orthogonality of the image "sources".

A limitation of BSS filtering techniques entails the required computational complexity, especially with 3D or high-frame-rate acquisitions. This could partly be dealt with by using a block-wise [17] or randomized SVD [28]. To further boost performance, integration of sparse basis selection [29] and robust principal component can be considered [30], [31], in which low-rank and sparse components are iteratively separated.

Even though its performance for *in-vivo* acquisitions remains to be investigated, the proposed methods show promise for adaptive clutter suppression. Future research should also be directed towards the nature of the threshold, that is, whether singular components could als be weighted or whether only consecutive singular components should be included. Moreover, the use of adaptive threshold definitions that change over time or with e.g. the cardiac cycle could be considered.

Acknowledgements

This research was conducted in the framework of the IMPULS2 program within the Eindhoven University in collaboration with Philips. This study was also funded by an unrestricted grant from the Dutch Cancer Society (#UVA2013-5941), and a Starting Grant from the European Research Council (#280209). We acknowledge also the Dutch TTW HTSM-13901 grant.

References

[1] O. Couture, V. Hingot, B. Heiles, P. Muleki-Seya, and M. Tanter, "Ultrasound Localization Microscopy and Super-Resolution: A State of the Art," *IEEE Transactions on Ultrasonics, Ferroelectrics, and Frequency Control*, vol. 65, no. 8, pp. 1304–1320, 2018.

[2] C. Errico, J. Pierre, S. Pezet, Y. Desailly, Z. Lenkei, O. Couture, and M. Tanter, "Ultrafast ultrasound localization microscopy for deep super-resolution vascular imaging," *Nature*, vol. 527, p. 499, nov 2015.

[3] E. Betzig, G. H. Patterson, R. Sougrat, O. W. Lindwasser, S. Olenych, J. S. Bonifacino, M. W. Davidson, J. Lippincott-Schwartz, and H. F. Hess, "Imaging Intracellular Fluorescent Proteins at Nanometer Resolution," *Science*, vol. 313, no. 5793, pp. 1642–1645, 2006.

[4] H. Geyer, G. Caracciolo, H. Abe, S. Wilansky, S. Carerj, F. Gentile, H.-J. Nesser, B. Khandheria, J. Narula, and P. P. Sengupta, "Assessment of Myocardial Mechanics Using Speckle Tracking Echocardiography: Fundamentals and Clinical Applications," *Journal of the American Society of Echocardiography*, vol. 23, no. 4, pp. 351–369, apr 2010.

[5] T. Kawagishi, "Speckle Tracking for Assessment of Cardiac Motion and Dyssynchrony," *Echocardiography*, vol. 25, no. 10, pp. 1167–1171, nov 2008.

[6] M. Lenge, A. Ramalli, E. Boni, H. Liebgott, C. Cachard, and P. Tortoli, "High-frame-rate 2-D vector blood flow imaging in the frequency domain," *IEEE Transactions on Ultrasonics, Ferroelectrics, and Frequency Control*, vol. 61, no. 9, pp. 1504–1514, 2014.

[7] F. Sammali, C. Blank, Y. Huang, N. Kuijsters, C. Rabotti, B. Schoot, and M. Mischi, "Dedicated ultrasound speckle tracking for quantitative analysis of uterine motion outside pregnancy," *IEEE Transactions on Ultrasonics, Ferroelectrics, and Frequency Control*, vol. 66, no. 3, pp. 581–590, 2018.

[8] S. Bjaerum, H. Torp, and K. Kristoffersen, "Clutter filter design for ultrasound color flow imaging," *IEEE transactions on ultrasonics, ferroelectrics, and frequency control*, vol. 49, no. 2, pp. 204–216, 2002.

[9] P. B. Calóope, F. N. S. Medeiros, R. C. P. Marques, and R. C. S. Costa, "A Comparison of Filters for Ultrasound Images," *Telecommunications and Networking*, pp. 1035–1040, 2004.

[10] C. Demené, T. Deffieux, M. Pernot, B. F. Osmanski, V. Biran, J. L. Gennisson, L. A. Sieu, A. Bergel, S. Franqui, J. M. Correas, I. Cohen, O. Baud, and M. Tanter, "Spatiotemporal Clutter Filtering of Ultrafast Ultrasound Data Highly Increases Doppler and fUltrasound Sensitivity," *IEEE Transactions on Medical Imaging*, vol. 34, no. 11, pp. 2271–2285, 2015.

[11] C. M. Gallippi, K. R. Nightingale, and G. E. Trahey, "BSS-based filtering of physiological and ARFI-induced tissue and blood motion," *Ultrasound in Medicine and Biology*, vol. 29, no. 11, pp. 1583–1592, 2003.

[12] F. W. Mauldin, D. Lin, and J. A. Hossack, "The singular value filter: a general filter design strategy for PCA-based signal separation in medical ultrasound imaging," *IEEE Transactions on Medical Imaging*, vol. 30, no. 11, pp. 1951–1964, 2011.

[13] F. Lin, J. K. Tsuruta, J. D. Rojas, and P. A. Dayton, "Optimizing Sensitivity of Ultrasound Contrast-Enhanced Super-Resolution Imaging by Tailoring Size Distribution of Microbubble Contrast Agent," *Ultrasound in medicine & biology*, vol. 43, no. 10, pp. 2488–2493, 2017.

[14] R. J. G. van Sloun, O. Solomon, Y. C. Eldar, H. Wijkstra, and M. Mischi, "Sparsity-driven super-resolution in clinical contrast-enhanced ultrasound," *Proceedings of IEEE International Ultrasonics Symposium*, pp. 1–4, 2017.

[15] R. J. G. van Sloun, O. Solomon, M. Bruce, Z. Z. Khaing, H. Wijkstra, Y. C. Eldar, and M. Mischi, "Super-resolution Ultrasound Localization Microscopy through Deep Learning," *arXiv preprint arXiv:1804.07661*, 2018.

[16] D. Ghosh, F. Xiong, S. R. Sirsi, P. W. Shaul, R. F. Mattrey, and K. Hoyt, "Toward optimization of in vivo super-resolution ultrasound imaging using size-selected microbubble contrast agents," *Medical Physics*, vol. 44, no. 12, pp. 6304–6313, oct 2017.

[17] P. Song, A. Manduca, J. D. Trzasko, and S. Chen, "Ultrasound Small Vessel Imaging With Block-Wise Adaptive Local Clutter Filtering," *IEEE Transactions on Medical Imaging*, vol. 36, no. 1, pp. 251–262, 2017.

[18] J. Baranger, B. Arnal, F. Perren, O. Baud, M. Tanter, and C. Demené, "Adaptive Spatiotemporal SVD Clutter Filtering for Ultrafast Doppler Imaging Using Similarity of Spatial Singular Vectors," *IEEE Transactions on Medical Imaging*, vol. 37, no. 7, pp. 1574–1586, 2018.

[19] G. H. Golub and C. Reinsch, "Singular value decomposition and least squares solutions," *Numerische mathematik*, vol. 14, no. 5, pp. 403–420, 1970.

[20] T. K. Moon and W. C. Stirling, *Mathematical Methods and Algorithms for Signal Processing*. New York, NY: Prentice Hall, Inc., 2000.

[21] J. Rissanen, "Modeling by shortest data description," *Automatica*, vol. 14, no. 5, pp. 465–471, 1978.

[22] V. A. Marčenko and L. A. Pastur, "Distribution of eigenvalues for some sets of random matrices," *Mathematics of the USSR-Sbornik*, vol. 1, no. 4, p. 457, 1967.

[23] Y. Desailly, A.-M. Tissier, J.-M. Correas, F. Wintzenrieth, M. Tanter, and O. Couture, "Contrast enhanced ultrasound by real-time spatiotemporal filtering of ultrafast images," *Physics in Medicine & Biology*, vol. 62, no. 1, p. 31, 2016.

[24] N. Hurley and S. Rickard, "Comparing measures of sparsity," *IEEE Transactions on Information Theory*, vol. 55, no. 10, pp. 4723–4741, 2009.

[25] A. R. Pries, T. W. Secomb, P. Gaehtgens, and J. F. Gross, "Blood flow in microvascular networks. Experiments and simulation." *Circulation research*, vol. 67, no. 4, pp. 826–834, 1990.

[26] B. Baillargeon, N. Rebelo, D. D. Fox, R. L. Taylor, and E. Kuhl, "The living heart project: a robust and integrative simulator for human heart function," *European Journal of Mechanics-A/Solids*, vol. 48, pp. 38–47, 2014.

[27] J.-Y. Bouguet, "Pyramidal implementation of the affine lucas kanade feature tracker description of the algorithm," *Intel Corporation*, vol. 5, no. 1-10, p. 4, 2001.

[28] P. Song, J. D. Trzasko, A. Manduca, B. Qiang, R. Kadirvel, D. F. Kallmes, and S. Chen, "Accelerated Singular Value-Based Ultrasound Blood Flow Clutter Filtering With Randomized Singular Value Decomposition and Randomized Spatial Downsampling," *IEEE transactions on ultrasonics, ferroelectrics, and frequency control*, vol. 64, no. 4, pp. 706–716, 2017.

[29] M. Zibulevsky and B. A. Pearlmutter, "Blind source separation by sparse decomposition in a signal dictionary," *Neural computation*, vol. 13, no. 4, pp. 863–882, 2001.

[30] M. Bayat and M. Fatemi, "Concurrent Clutter and Noise Suppression via Low Rank Plus Sparse Optimization for Non-Contrast Ultrasound Flow Doppler Processing in Microvasculature," *Proceedings of the IEEE International Conference on Acoustics, Speech and Signal Processing*, pp. 1080–1084, 2018.

[31] O. Solomon, R. Cohen, Y. Zhang, Y. Yang, Q. He, J. Luo, R. J. G. van Sloun, and Y. C. Eldar, "Deep Unfolded Robust PCA with Application to Clutter Suppression in Ultrasound," *IEEE Transactions on Medical Imaging*, p. 1, 2019.